IOSR Journal of Engineering (IOSRJEN) **www.iosrjen.org**
ISSN (e): 2250-3021, ISSN (p): 2278-8719
Vol. 09, Issue 4 (April. 2019), ||S (I) || PP 01-09

Modelling of Quasi-Brittle Fractures in Gradient Particular Composites

PuziZhang[1], JinxingLiu[1]
[1]*Faculty of Civil Engineering and Mechanics, Jiangsu University, Xuefu Road 301, Zhenjiang, Jiangsu Province, China, postal code: 212013*
Corresponding Author: Jinxing Liu

Abstract: The microstructure of the gradient particular composites plays an important role in their fracture behaviour. The distribution of particles is ruled by a prescribed gradient of particle volume fraction. In this paper, the generalized beam (GB) lattice is used to simulate the damage and fracture of gradient particular composites. The compression and tension simulations of two different gradient particular materials are performed. The effects of the gradient distribution of particles on the fracture process are discussed in detail.

Keywords: Gradient particular composites, Generalized Beam (GB) Lattice Model, Quasi-brittle Fracture.

Date of Submission: 26-03-2019 Date of acceptance: 09-04-2019

I. INTRODUCTION

The microstructure of particle composites in terms of particle size, shape, distribution and so on, plays an important role in the fracture behaviour[1]. Gradient particular composites are different from traditional particle counterparts, because the particles embedded to the matrix are no longer randomly distributed,but in a certain gradient along the required direction[2]. In the research field of the damage and fracture mechanics of particle composite materials, many scholars have carried out fruitful works. Mishnaevsky et al. [3] studied the effect of particle distribution, quantity and particle size on the mechanical properties of composites in aluminium-based silicon carbide particle composites. In particular, the ultimate strain of the cluster silicon carbide particles is significantly lower than the ultimate strain of uniform random silicon carbide particles. Zhang et al.[4] established a new three-dimensional mesostructured finite element model to predict the elastoplastic response and fracture behaviour of aluminium-based silicon carbide particles. The numerical results provided a basis of studying the damage mechanism of aluminium-based silicon carbide particle composites, and the effects of interface strength and particle strength on the properties of composites were discussed in detail. Generally, in the finite element modelling of particle composite materials, it is indispensable to simplify the meso-structure. Chawla et al.[5] performed continuous sectioning the particle composites and then used finite element simulation to model the three-dimensional microstructure of the particle-reinforced metal matrix composite. The biggest advantage of this method is that it can realistically model the shape of the particles, so the results of the simulation are more accurate than the results of the simplified modelling. However, the dominant form of the deformation in metal-based particle reinforced composites is plastic deformation, which has a relatively pronounced stage of plastic deformation after peak loading. The research content of this paper is to build up the reinforcing particles in the brittle matrix and study the quasi-brittle fracture of the gradient particular composites.

The influence of the microstructure in the particle composite on the damage mechanism and fracture process is very profound[6]. The gradient distribution of particles obviously has a considerable influence on the macroscopic mechanical properties and mesoscopic damage mechanism of the composite[7]. For example, in the structural analysis for the quasi-brittle materialslike concrete, a homogeneous cross-section, is generally assumed in terms of strength and mechanical properties. In fact, concrete is a composite of cement matrix and coarse aggregates. Therefore, the actual composition of the concrete members is unlikely to remain homogeneous within any arbitrary cross section. The coarse aggregate will come denser in the lower part of the component due to gravity, resulting in a gradient distribution in strength, modulus of elasticity and Poisson's ratio across the cross-section of the material. Gan et al.[8] used experimental methods to study the fracture characteristics of specimens with two different strength concretes combined under compression conditions. The analysis indicated that the cracking and failure of the lower strength concrete part is a sign of the strength of the entire grading material, so the relative difference between the strength of the composite material has a negative impact on the overall mechanical properties of the concrete. Microcracks are generated prematurely in the weaker layers, causing stress to concentrate in the corresponding layers. In order to overcome this problem, the

mechanical properties of the material should be changed more smoothly, so that the stress transfer inside the material does not cause a severe stress concentration in anextremely thin layer. Adding reinforcing particles according a prescribed distribution gradient is one way to achieve this change in the mechanical properties of the composite. Based on the generalized beam lattice model, this paper improves the particle modelling method to realize the gradient distribution of particles, and obtains the reaction-displacement curves and crack patterns of the corresponding specimens under different particle gradient distribution modes.

II. MODEL DESCRIPTION

2.1 GB lattice model

The generalized beam (GB) lattice model was proposed by Liu et al.[9-13] for simulating the fracture process in the quasi-brittle materials like concrete. Each element can be composed of three beams with independent material properties. The response of beams can be described by the generalized force of its two ends (Fig. 1),

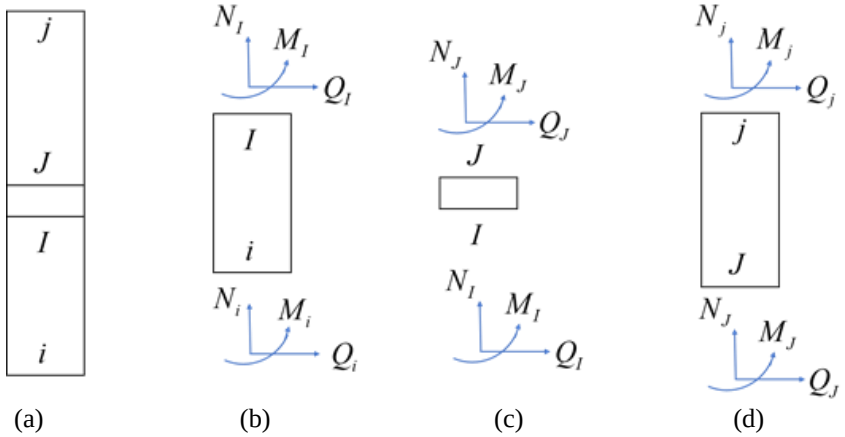

(a) (b) (c) (d)

Figure 1: Kinetics and statics of a GB lattice element.

$$\begin{Bmatrix} Q_1 \\ N_1 \\ M_1 \\ Q_2 \\ N_2 \\ M_2 \end{Bmatrix} = \underbrace{\begin{bmatrix} M_{11} & 0 & -M_{34} & -M_{11} & 0 & -M_{34} \\ & M_{22} & 0 & 0 & -M_{22} & 0 \\ & & M_{33} & M_{34} & 0 & M_{36} \\ & & & M_{11} & 0 & M_{34} \\ & & SYM & & M_{22} & 0 \\ & & & & & M_{33} \end{bmatrix}}_{M} \begin{Bmatrix} u_1 \\ v_1 \\ \varphi_1 \\ u_2 \\ v_2 \\ \varphi_2 \end{Bmatrix} \tag{1}$$

where $F_{12}=\{Q_1 \quad N_1 \quad M_1 \quad Q_2 \quad N_2 \quad M_2\}^T$ and $u_{12}=\{u_1 \quad v_1 \quad \varphi_1 \quad u_2 \quad v_2 \quad \varphi_2\}^T$ are the generalized force vector and the generalized displacement vector, and M_{ij} are assigned values based on the theory on the theory of the Euler-Bernoulli or Timoshenko beam. In the local coordinate system on each element ij, the y-axis points from end i and j, and the x-axis is determined by rotating y-axis 90° clockwise.The material and geometrical properties of lattice elements are calibrated based on the equivalence of strain energy[14].

Mohr-coulomb criterion is a mathematical model describing the response of materials such as concrete to shear stress as well as normal stress. The criterion with tension and compression cut-offs are shown in Fig. 2 and can be expressed by the following inequations:

$$\begin{gathered} \sigma < f_t \\ |t| < c - \sigma \tan\phi \\ \sigma > -f_c \end{gathered} \tag{2}$$

where c is the cohesive strength and ϕ is the friction angle, τ and σ are the shear stress and the normal stress, f_t and f_c are the tensile and compressive strengths. The normal stress can be written as:

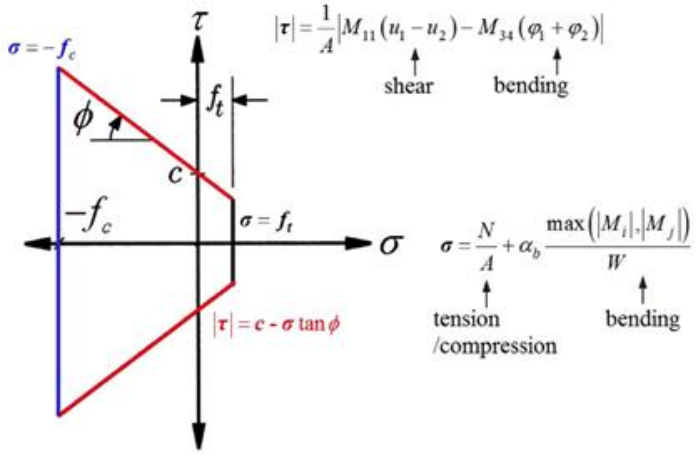

Figure 2: Mohr-Coulomb rule with a tension and compression cut-off as the failure criterion[12].

$$\sigma = \frac{N}{A} + \alpha_b \frac{\max(|M_i|, |M_j|)}{W} \tag{3}$$

where N is the normal force, M_i and M_j are the bending moments at node i and j, W is the section modulus, the coefficient α_b regulates what part of the bending moment is considered. While the shear stress can be calculated as:

$$|\tau| = \frac{1}{A}|M_{11}(u_1 - u_2) - M_{34}(\varphi_1 + \varphi_2)| \tag{4}$$

and A is the area of the cross-section.

2.2 Distribution form of gradient particle

For the research in this paper, by improving the particle distribution mechanism, the particles are embedded to the matrix according to a certain gradient. According to the concept of gradient materials, gradient particular composites can be divided into the following two categories:

1. Gradient change in particle size.
2. Gradient change in particle content.

For the first kind, the gradient of the particle size can be achieved by placing different sizes of particles in one direction (Fig. 3a). For the second, the particle content changes in a gradient, which can be varied by distance in the direction of the particle in one direction of the lattice (Fig. 3b).

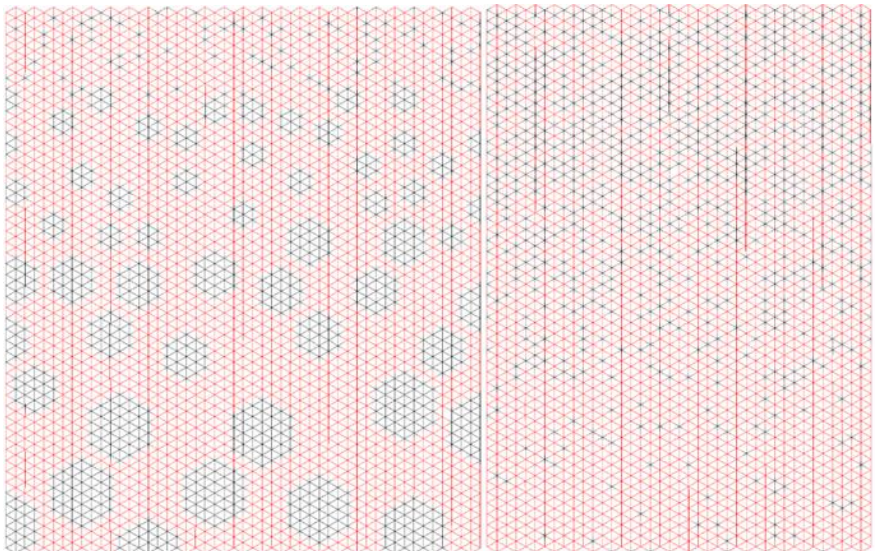

(a) (b)

Figure 3: Distribution form of gradient particle. (a) Gradient change in particle size; (b) Gradient change in particle content.

III. NUMERICAL EXAMPLE AND ANALYSES

3.1 Gradient change in particle size

The compression tests are performed on a GB lattice with a rectangular geometry of 7.5 by 9 cm. The employed lattice includes 9043 GB elements and 3085 nodes. All elements are $\sqrt{3}/10$ cm. The lower boundary of the model is fixed, and a uniform control displacement is applied to the upper boundary. In order to study the effect of particle size change on the macroscopic mechanical properties and fracture morphology of the material, a total of six simulation experiments were carried out, including a set of random particle distribution test.

Table 1. Meso elastic and strength properties of the material

Phases	E (MPa)	f_c (MPa)	f_t (MPa)	c (MPa)	ϕ ($^\circ$)	D
Matrix	25,000	60.0	5.0	7.5	45	0.9
Interface	25,000	15.0	2.7	1.875	45	0.9
Aggregate	70,000	120.0	10.0	15.0	45	0.9

The first case, i.e. “Gradient”, has the following settings:

a. Refer to the data in Table 1 for the parameters related to material elasticity and strength in “Gradient”.
b. The strength of the matrix at the upper and lower boundaries of the model is enhanced. The compressive load applied at the upper boundary is quasit-static loading.
c. The left and right boundaries of the geometric model do not impose and constraints.
d. The geometric model contains a total of 154 particles of different sizes. The distribution of the particles in the test is shown in Table 2.

Table 2. The gradient distribution of particles in the specimen

Height from the upper boundary	Interlayer thickness	Number of particles
0.0cm	0.9cm	80
0.9cm	3.6cm	40
4.5cm	3.6cm	30
8.1cm	0.9cm	4

The second “Random” specimen has the same settings as the first “Gradient” specimen, but the particles are randomly distributed in the matrix.

The third “Gradient [2]” specimen has the same settings as the first “Gradient” specimen, but the number of particles in the second layer was adjusted, adding 20 particles.

The fourth “Gradient [2’]” specimen has the same setting as the first “Gradient” specimen, but the number of particles in the second layer was adjusted, adding 10 particles.

The fifth “Gradient [3]” specimen has the same setting as the first “Gradient” specimen, but the number of particles in the third layer was adjusted, reducing 15 particles.

The sixth “Gradient [3’]” specimen has the same setting as the first “Gradient” specimen, but the number of particles in the third layer was adjusted, reducing 10 particles.

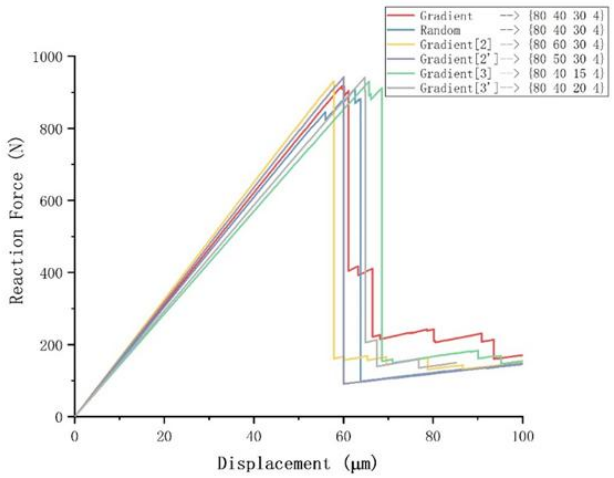

(a)

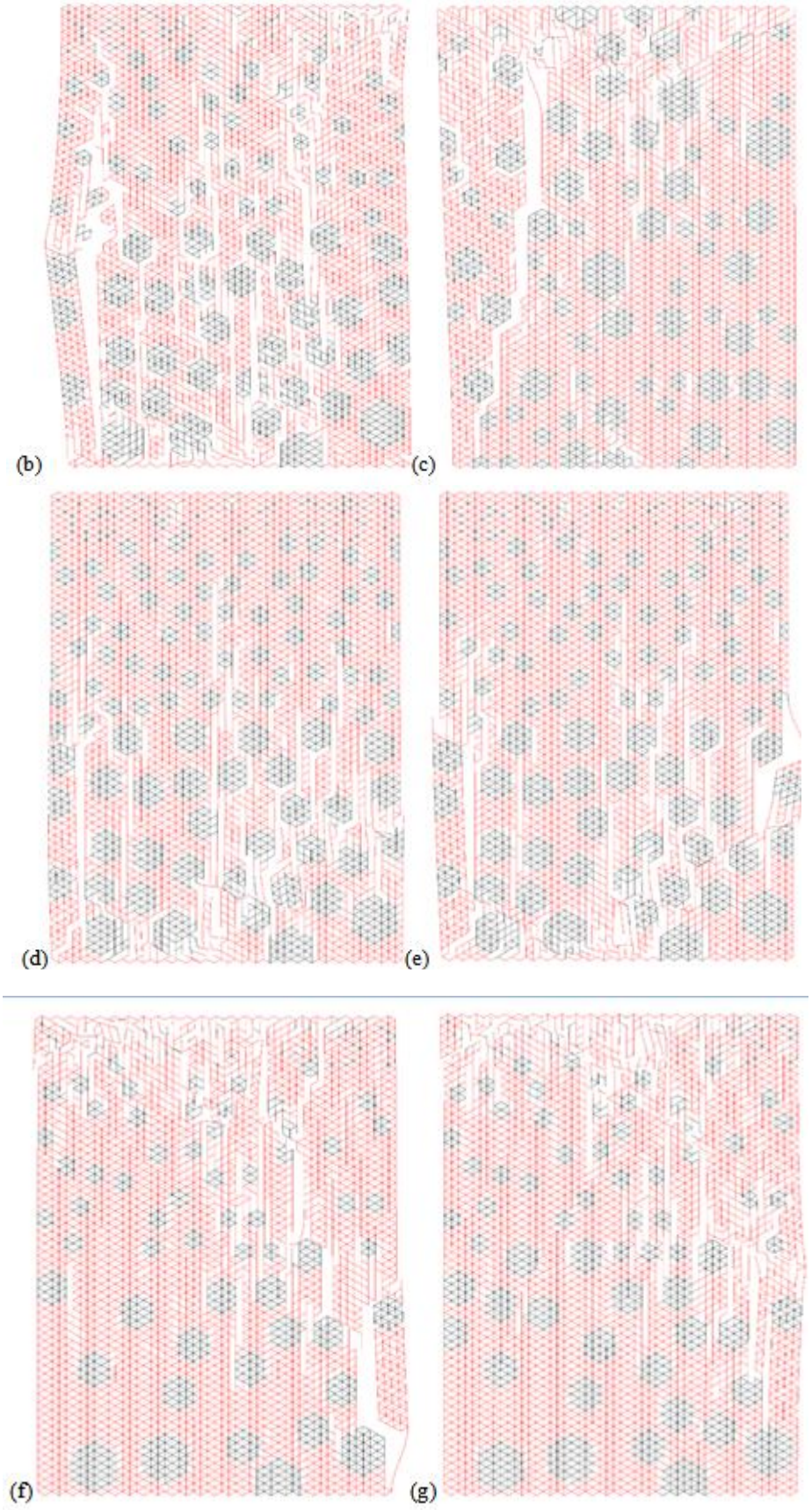

Figure 4: (a) Diagrams of reaction force versus the controlled displacement. Crack patterns corresponding to the controlled displacement. (b) 61.1 μm in "Gradient"; (c) 77.1 μm in "Random"; (d) 57.8 μm in "Gradient [2]"; (e) 60.1 μm in "Gradient [2']"; (f) 68.5 μm in "Gradient [3]"; (g) 64.4 μm in "Gradient [3']".

The simulation results are shown in Fig. 4. The peak force of the first "Gradient" specimen is 904N, and the peak force of the second "Random" specimen is 882N. "Gradient" specimen become critical earlier than "Random" specimen and has better ductility at post-peak area. The pre-peak behavior in both cases is similar. As the external load increases, the number of element fractures continues to accumulate, and no serious macroscopic cracks appear. After the "Random" specimen's peak, that is, after the macro crack occurs, the corresponding reaction force drops sharply, and the number of broken cells suddenly increases. However, in the "Gradient" specimen, the initial damage occurred in the middle part of the specimen, and a number of macroscopic cracks gradually appeared in the specimen after the peak. Furthermore, it can be seen from the results of the simulation of the six specimens that an increase in the number of particles in the gradient particular composites causes the peak load of the specimen to appear earlier. The main factor leading to this phenomenon is that more particles will produce more interfaces. The weak interface is still the main factor causing the damage and fracture of the gradient particular composites. Since the "Gradient [2]" and "Gradient [2']" specimens increase the number of particles in a position closer to the upper boundary, this region first causes microcracks. As the control displacement increase, the microcracks gradually merge, and when macroscopic cracks appear, the cracks expend toward the weaker lower boundary. As a result, the crack patterns under the peak loads of these two specimens show numerous scattered cracks in the lower region. The "Gradient [3]" and "Gradient [3']" specimens reduce the particles in a range closer to the lower boundary, which is equivalent to the strengthening of this region. When the micro-cracks in the area gradually merge to form a macro-crack, the direction expands toward the weaker upper layer, which eventually leads to the dispersion of the crack pattern under the peak load of the specimen in the region closer to the upper boundary.

3.2 Gradient change in particle content

The horizontal tensile tests are performed on a GB lattice with a rectangular geometry of 22.5 by 22.5 cm. All elements are $\sqrt{3}/10\,\text{cm}$. The left boundary of the model is fixed, and a uniform control displacement is applied to the right boundary. The parameters related to material elasticity and strength in the specimens are referred to the data in Table 1 unless otherwise specified. The employed lattice includes 67574 GB elements and 22725 nodes. The first three specimens were pure gradient particular composites. The latter two specimens contain a gradient particle layer and a random particle layer. The interface strength of the first three specimens is $f_t = 1.0Mpa$. The interface strength of Group 4 strong interface and Group 5 strong interface is $f_t = 2.0Mpa$. The particle content is shown in the Table 3 and Table 4:

Table 3. Particle gradient form from Group 1 to Group 3

Height	Span	Content: Group 1	Content: Group 2	Content: Group 3
9cm	9cm	70%	90%	80%
13.5cm	4.5cm	50%	50%	50%
22.5cm	9cm	30%	10%	20%

Table 4. Particle gradient form of Group 4 and Group 5

Height	Span	Content: Group 4	Content: Group 5
2.25cm	2.25cm	70%	70%
2.5cm	2.25cm	50%	40%
6.75cm	2.25cm	30%	10%
22.5cm	15.75cm	—Random particle area, contains 140 particles	

The simulation results from Group 1 to Group 3 are shown in Fig. 5. It can be seen from the reaction force-displacement curves that the pure gradient particular composites have a relatively large ductility in the post-peak region when the interface is weak. Combined with the fracture patterns of three sets of specimens, it can be seen that the more severe the gradient of the particles, the temporary change of the crack propagation direction in the excessive region of different particle content, that is, the post-peak region in the corresponding reaction-displacement curve. The platform on which the reaction curve appears. As the control displacement gradually increases, the crack continues to expand along the gradient direction, and reverses when the next particle content is excessive. As the control displacement continues to increase, the expansion direction returns to the direction parallel to the gradient until the specimen was completely broken.

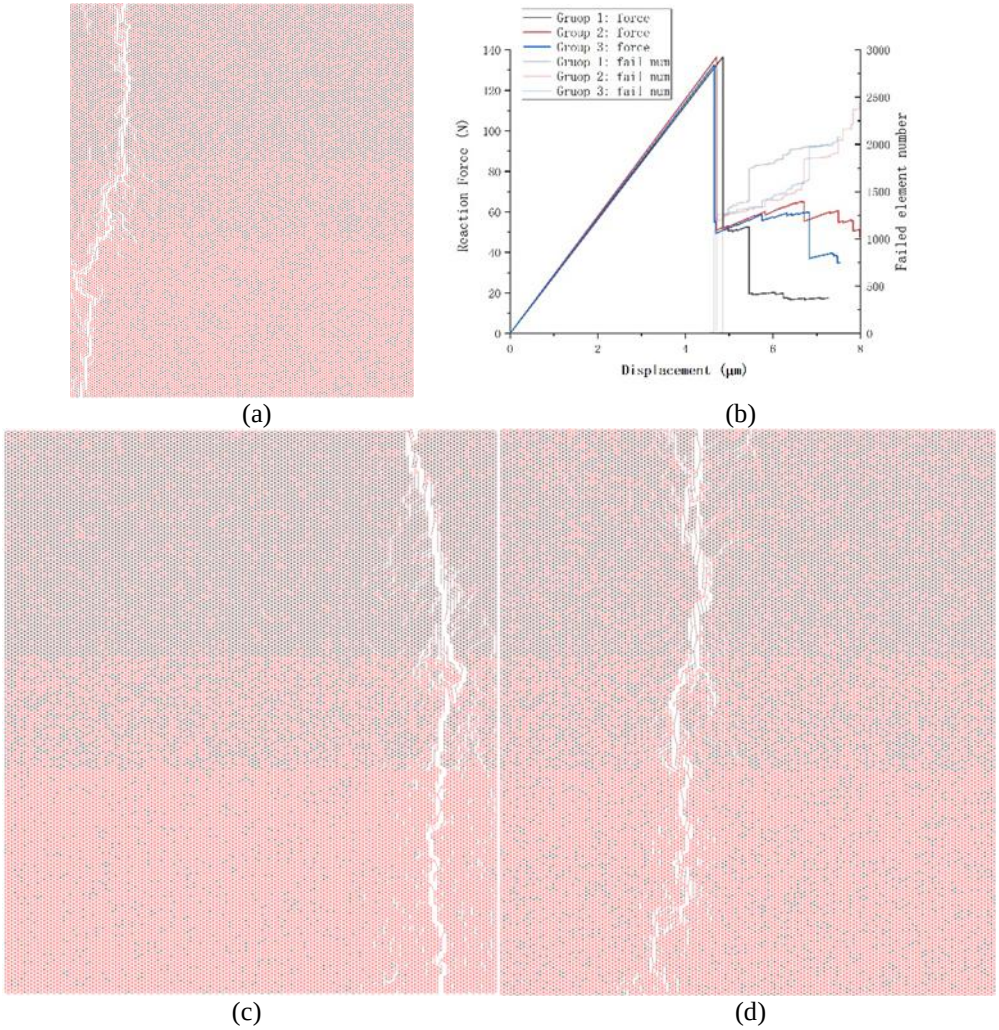

Figure 5: Results of Group 1, Group 2 and Group 3. (a) Diagrams of reaction force versus the controlled displacement. Crack patterns corresponding to the controlled displacement (b) 5.5 μm in Group 1; (c) 8.0 μm in Group 2; (d) 7.3 μm in Group 3.

The simulation results of Group 4 and Group 5 are shown in Fig. 6. It can be seen from the reaction force-displacement curve that the ductility of the composite is mainly due to the weak interface, which causes more scattered cracks. When the load increases to a certain critical value, the dispersed cracks merge to form macroscopic cracks. The macroscopic cracks continue to expand in the direction of the gradient and continue to form many microcracks around the macroscopic crack. This phenomenon is not obvious when the interface is strong. However, a weaker interface results in a lower peak load and corresponding control displacement of the composite. As the same time, it can be seen from the fracture patterns of the groups of weaker specimens that when the interface is weak, the cracks in the random particle layer are more dispersed. Macroscopic cracks cannot be formed in the random particle layer before macroscopic cracks are formed in the gradient layer. The final macroscopic cracks generated within the gradient layer.

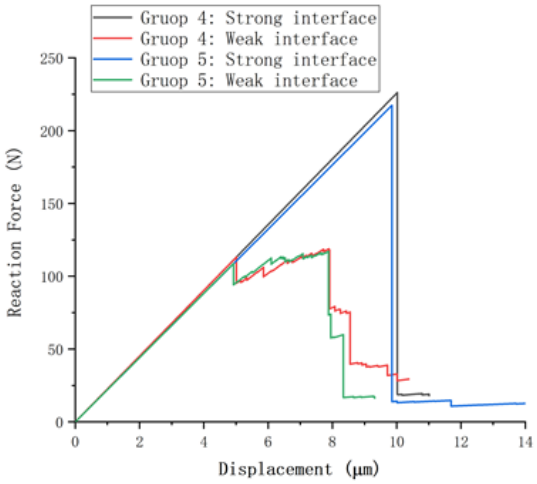

(a)

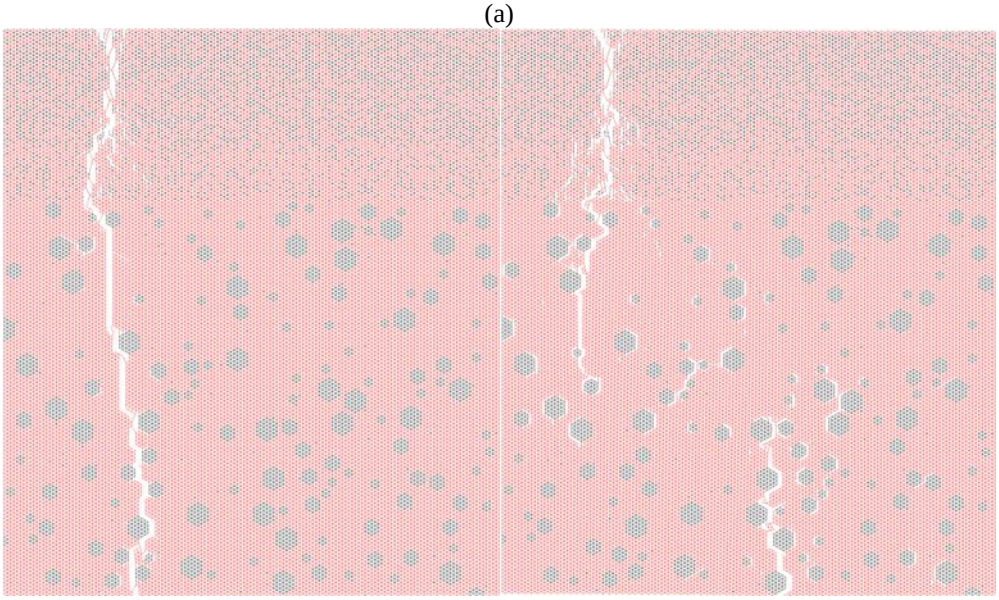

(b) (c)

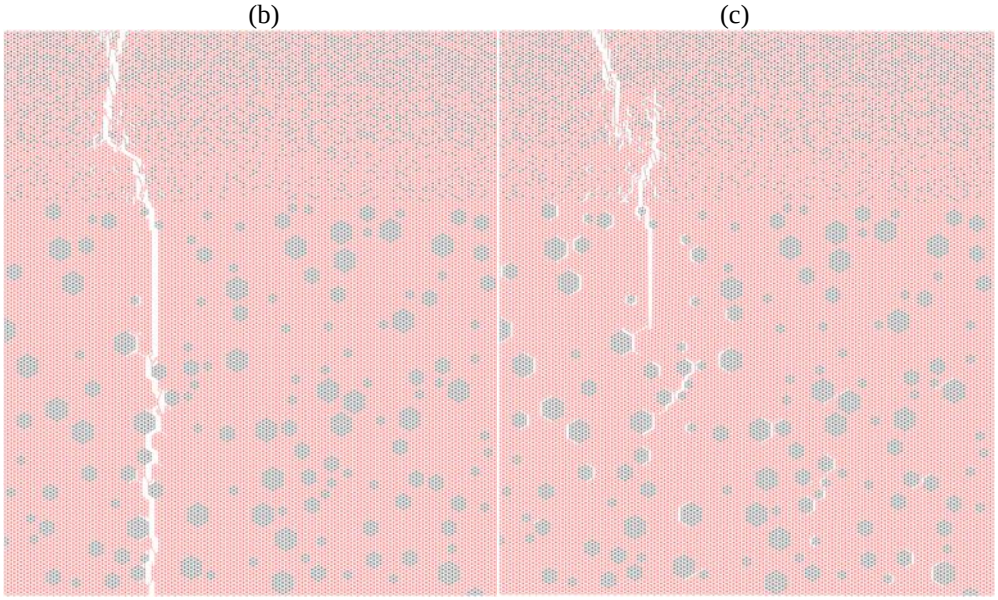

(d) (e)

Figure 6: Results of Group 4 and Group 5. (a) Diagrams of reaction force versus the controlled displacement. Crack patterns corresponding to the controlled displacement (b) 10.0 μm in Group 4 (Strong interface); (c) 9.1 μm in Group 4 (Weak interface); (d) 9.8 μm in Group 5 (Strong interface); (e) 7.8 μm in Group (Weak interface).

IV. CONCLUSION

In this paper, the generalized beam lattice model is modified to simulate failures in gradient particular composites. For two typical materials, the failure processesare simulated, and the reaction force-displacement curves and the corresponding crack patterns are analyzed. The results show that the gradient particularcomposites have better ductility than the conventional ones. Gradient of particle distributions is found to strongly influence the ductility, peak load as well as on crack propagation.

REFERENCES

[1]. J.E. Bolander, N. Sukumar, Irregular lattice model for quasistatic crack propagation. Physical Review B. 20(9) (2005), 4106.
[2]. A. Kawasaki, R.J.E.F.M. Watanabe, Thermal fracture behavior of metal/ceramic functionally graded materials. Engineering Fracture Mechanics. 69(14) (2002), 1713-1728.
[3]. L.M. Jr, et al., Effect of microstructure of particle reinforced composites on the damage evolution: probabilistic and numerical analysis. 64(12) (2004), 1805-1818.
[4]. Z. Jie, et al., 3D Microstructure-based finite element modeling of deformation and fracture of SiCp/Al composites. 123 (2016), 1-9.
[5]. CHAWLA, et al., Three-dimensional visualization and microstructure-based modeling of deformation in particle-reinforced composites. 54(6) (2006), 1541-1548.
[6]. G. Lilliu, J.G.M. van Mier, On the relative use of micro-mechanical lattice analysis of 3-phase particle composites. Engineering Fracture Mechanics. 74(7) (2007), 1174-1189.
[7]. Y.C. Tsui, S.J. Howard, T.W.J.A.M.E.M. Clyne, The effect of residual stresses on the debonding of coatings—II. An experimental study of a thermally sprayed system. 42(8) (1994), 2837-2844.
[8]. B.S. Gan, A. Han, M.M.A.J.P.E. Pratama, The Behavior of Graded Concrete, an Experimental Study ☆. 125 (2015), 885-891.
[9]. J.X. Liu, Z.T. Chen, K.C. Li, A 2-D lattice model for simulating the failure of paper. Theoretical and Applied Fracture Mechanics. 54(1) (2010), 1-10.
[10]. J.X. Liu, N.G. Liang, Algorithm for simulating fracture processes in concrete by lattice modeling. Theoretical and Applied Fracture Mechanics. 52(1) (2009), 26-39.
[11]. J.X. Liu, et al., Lattice type of fracture model for concrete. Theoretical and Applied Fracture Mechanics. 48(3) (2007), 269-284.
[12]. J.X. Liu, N.G. Liang, A.K.J.A.M.M. Soh, Modeling of progressive failures in quasi-brittle media based on a temporal stress-redistribution mechanism. (2019), 464-488.
[13]. J.X. Liu, et al., Modified generalized beam lattice model associated with fracture of reinforced fiber/particle composites. Theoretical and Applied Fracture Mechanics. 50(2) (2008), 132-141.
[14]. B.L. Karihaloo, P.F. Shao, Q.Z. Xiao, Lattice modelling of the failure of particle composites. Engineering Fracture Mechanics. 70(17) (2003), 2385-2406.

IOSR Journal of Engineering (IOSRJEN) is UGC approved Journal with Sl. No. 3240, Journal no. 48995.

PuziZhang. "Modelling Of Quasi-Brittle Fracturesin Gradient Particular Composites." IOSR Journal of Engineering (IOSRJEN), vol. 09, no. 04, 2019, pp. 01-09.